Deletion of exons 9 and 10 of the Presenilin 1 gene in a patient with Early-onset Alzheimer Disease generates longer amyloid seeds

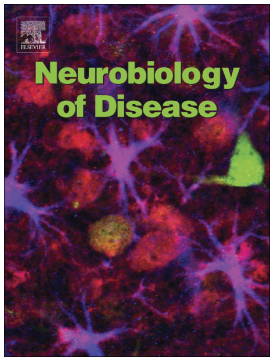

Kilan Le Guennec, Sarah Veugelen, Olivier Quenez, Maria Szaruga, Stéphane Rousseau, Gaël Nicolas, David Wallon, Frédérique Fluchere, Thierry Frébourg, Bart De Strooper, Dominique Campion, Lucía Chávez-Gutiérrez, Anne Rovelet-Lecrux

PII: S0969-9961(17)30102-X
DOI: doi: 10.1016/j.nbd.2017.04.020
Reference: YNBDI 3951

To appear in: *Neurobiology of Disease*

Received date: 19 January 2017
Revised date: 27 March 2017
Accepted date: 27 April 2017

Please cite this article as: Kilan Le Guennec, Sarah Veugelen, Olivier Quenez, Maria Szaruga, Stéphane Rousseau, Gaël Nicolas, David Wallon, Frédérique Fluchere, Thierry Frébourg, Bart De Strooper, Dominique Campion, Lucía Chávez-Gutiérrez, Anne Rovelet-Lecrux , Deletion of exons 9 and 10 of the Presenilin 1 gene in a patient with Early-onset Alzheimer Disease generates longer amyloid seeds. The address for the corresponding author was captured as affiliation for all authors. Please check if appropriate. Ynbdi(2017), doi: 10.1016/j.nbd.2017.04.020

Deletion of exons 9 and 10 of the Presenilin 1 gene in a patient with Early-Onset Alzheimer Disease generates longer amyloid seeds.

Kilan Le Guennec[1], Sarah Veugelen[2,3], Olivier Quenez[1], Maria Szaruga[2,3], Stéphane Rousseau[1], Gaël Nicolas[1], David Wallon[4], Frédérique Fluchere[5], Thierry Frébourg[6], Bart De Strooper[2,3,7], Dominique Campion[1,8], Lucía Chávez-Gutiérrez[2,3], Anne Rovelet-Lecrux[1].

[1]Normandie Univ, UNIROUEN, Inserm U1245 and Rouen University Hospital, Department of Genetics and CNR-MAJ, F 76000, Normandy Center for Genomic and Personalized Medicine, Rouen, France

[2]VIB- Center for Brain and Disease Research, University of Leuven, 3000 Leuven, Belgium

[3]Center for Human Genetics and Leuven Research Institute for Neuroscience & Disease (LIND), University of Leuven, 3000 Leuven Belgium

[4]Normandie Univ, UNIROUEN, Inserm U1245 and Rouen University Hospital, Department of Neurology and CNR-MAJ, F 76000, Normandy Center for Genomic and Personalized Medicine, Rouen, France

[5]Department of Neurology and Movement Disorders, APHM, La Timone, Pôle de Neurosciences cliniques, Aix-Marseille Univ, Marseille, France.

[6]Normandie Univ, UNIROUEN, Inserm U1245 and Rouen University Hospital, Department of Genetics, F 76000, Normandy Center for Genomic and Personalized Medicine, Rouen, France

[7]Institute of Neurology, University College London, Queen Square, WC1N 3BG London, UK

[8]Department of Research, Rouvray Psychiatric Hospital, Sotteville-lès-Rouen, France

Corresponding author:

Anne Rovelet-Lecrux, anne.roveletlecrux@univ-rouen.fr

Abstract

Presenilin 1 (*PSEN1*) mutations are the main cause of autosomal dominant early onset Alzheimer Disease (EOAD). Among them, deletions of exon 9 have been reported to be associated with a phenotype of spastic paraparesis.

Using exome data from a large sample of 522 EOAD cases and 584 controls to search for genomic copy-number variations (CNVs), we report here a novel partial, in-frame deletion of *PSEN1*, removing both exons 9 and 10. The patient presented with memory impairment associated with spastic paraparesis, both starting from the age of 56 years. He presented a positive family history of EOAD. We performed functional analysis to elucidate the impact of this novel deletion on PSEN1 activity as part of the γ-secretase complex. The deletion does not affect the assembly of a mature protease complex but has an extreme impact on its global endopeptidase activity. The mutant carboxypeptidase-like activity is also strongly impaired and the deleterious mutant effect leads to an incomplete digestion of long Aβ peptides and enhances the production of Aβ43, which has been shown to be potently amyloidogenic and neurotoxic *in vivo.*

Keywords

Alzheimer Disease; early-onset; PSEN1; hydrophilic loop; Aβ43; amyloid.

Introduction:

Mutations in the *Amyloid Precursor protein* (*APP*), *Presenilin 1* (*PSEN1*) and *Presenilin 2* (*PSEN2*) genes and duplications of the *APP* locus are the main causes of Autosomal Dominant Early-onset Alzheimer's disease (AD-EOAD). Mutations in the *PSEN1* gene account for the majority of AD-EOAD cases with 221 pathogenic mutations reported to date (http://www.alzforum.org/), including 6 deletions of *PSEN1* exon 9 resulting either from splicing mutations (Perez-Tur et al., 1995; Sato et al., 1998; Rovelet-Lecrux et al., 2015) or genomic deletions (Prihar et al., 1999; Hiltunen et al., 2000; Smith et al., 2001).

Presenilin is the catalytic subunit of the γ-secretase, an enzymatic complex involved in the processing of numerous type 1 transmembrane proteins, including APP and Notch (Jurisch-Yaksi et al., 2013). The sequential cleavage of APP by the β- and γ-secretase releases the Aβ peptides of different lengths. The accumulation of aggregation-prone Aβ peptides into senile plaques is central to AD pathophysiology. The γ-secretase cleavage occurs in a multi-step process: first, the endopeptidase (ε) cleavage releases the C-terminal part of APP (AICD) and, depending on the position of the ε-cleavage, either the Aβ49 or Aβ48 fragment will be produced. Then, carboxypeptidase-like γ-cleavages sequentially shorten these Aβ peptides following specific lines of production: Aβ49->Aβ46->Aβ43->Aβ40->Aβ37 and Aβ48->Aβ45->Aβ42->Aβ38 (Takami et al., 2009). AD-linked *PSEN1* variations result in various effects on γ-secretase activity: whereas the endopeptidase cleavage is not always impaired, the carboxypeptidase efficiency is consistently reduced, resulting in qualitative shifts in Aβ profile, favoring the secretion of longer, more aggregation-prone Aβ peptides such as Aβ42 and Aβ43, and possibly longer (Saito et al., 2011; Chávez-Gutiérrez et al., 2012; Szaruga et al., 2015; Veugelen et al., 2016).

In the present study, we used exome sequencing data from a large cohort of 522 EOAD cases and 584 controls to search for genomic copy-number variations (CNVs). We identified a novel mutation consisting of a genomic deletion of exons 9 and 10 of *PSEN1* in an EOAD patient and evaluated the consequences of this variation on γ-secretase activity. The deletion of exons 9-10 drastically decreases the global endopeptidase activity and results in an increased secretion of Aβ43. Following previous work demonstrating that other highly inactivating *PSEN1* mutations show similar effects on Aβ secretion (Veugelen et al., 2016), the data presented here further supports the pathogenic role of Aβ43, even at low concentrations.

MATERIALS AND METHODS

Patients, whole exome sequencing, and CNV calling

We performed whole exome sequencing (WES) in 546 patients with EOAD and 597 controls from French ancestry. Inclusion of patients and controls, WES details, bioinformatics pipelines and quality checks (QC) were previously reported (Nicolas et al., 2016b). Briefly, diagnoses of probable AD were performed according to the NIA-AA recommendations **(McKhann et al., 2011) and genetic diagnosis of mutation in AD-causative genes were first made prior to WES if our national criteria were met (*i.e.* two cases from the same family with AAO before 65 or sporadic case with AAO before 50) (Nicolas et al., 2016a). Screening of AD-causative CNVs was routinely performed for *APP* duplication following same criteria.**

For 385 EOAD patients, cerebrospinal fluid (CSF) total-Tau, Phosphorylated-Tau, and Aβ42 biomarkers were available and were all indicative of AD pathophysiology (Le Guennec et al., 2016a). The mean age at onset was 55 years (range 44-65). Out of the 546 initially included

cases and 597 controls, 535 cases and 593 controls passed the QC for genetic case-control association analyses and were retained for CNV calling.

CNV calling was performed using the CANOES software (Backenroth et al., 2014), an algorithm dedicated to the detection of quantitative genomic variations based on read depth information. A final sample of 522 patients and 584 controls passed the quality criteria for CNV calling. **A total of 13,870 CNVs were called in these 1106 samples. Note that, as CNV calling by CANOES is based on read depth, only rare events are efficiently detected. Previous validation of this software using aCGH data revealed a high concordance (88%) between the two methods, and showed that CANOES specifically missed a subset of very small monoexonic CNVs with lower read depth (Le Guennec et al., 2016b).**

Quantitative Multiplex PCR of Short Fluorescent Fragments (QMPSF)

Genomic DNA was extracted from blood samples using the Flexigen DNA kit (Qiagen, Hilden, Germany). ***PSEN1*** **exon 9/10 deletion was validated according to an already published process using QMPSF spanning exons 1, 7 and 18 of** ***APP*** **(Rovelet-Lecrux et al., 2006) to which we added two supplemental amplicons spanning exons 9 and 10 of** ***PSEN1*****.** Primers are available upon request. DNA fragments were then separated on an ABI 3500 genetic analyzer. The fluorescence profiles were analyzed using the GeneMapper software 5 (Applied Biosystems).

Breakpoint sequencing

After delineation of the deletion by QMPSF using amplicons located in introns 8 and 10 of *PSEN1*, the rearranged allele was PCR-amplified and Sanger sequenced using the following primers: F-5'-AGTGTATTGCCTGCCTGGTTTC-3' and R-5'-

CTGGCTGTTGCTGAGGCTTT-3'. DNA sequences were run on an ABI 3500 genetic analyzer and analyzed using the Sequencing Analysis Software 6 (Applied Biosystems).

RT-PCR analysis

Total RNA was extracted from whole blood collected into PAXgene Blood RNA tubes using the PAXgene Blood RNA kit (Qiagen, Hilden, Germany). RNA was reverse-transcribed using the Verso cDNA synthesis kit (Fisher Scientific, Illkirch, France) with a blend of random hexamers and anchored oligo-dT (3:1). The cDNA were then PCR-amplified using the following primers: F-5'-GTGGCTGTTTTGTGTCCGAA-3' and R-5'-TGGTTGTGTTCCAGTCTCCA-3'. Fragments were separated on a 2% agarose gel and extracted using the Nucleospin gel and PCR clean up (Macherey-Nagel, Düren, Germany). The resulting PCR products were sequenced and run on an ABI 3500 genetic analyzer and analyzed using the Sequencing Analysis Software 6 (Applied Biosystems).

Antibodies

Mouse PEN-2 was detected using a polyclonal antibody (B126.2, RRID:AB_2571520) and mouse Nicastrin was detected using the monoclonal antibody 9C3 (RRID:AB_2571521), as previously described (Chávez-Gutiérrez et al., 2012). Human PSEN1-NTF (RRID: AB_11215630) and PSEN1-CTF (RRID:AB_95175) were detected using monoclonal antibodies MAB1563 (Chemicon) and MAB5232 (Millipore/Chemicon), respectively. AICD was detected using the APP C-terminus antibody B63.3.

Generation of stable cell lines

Psen1/Psen2 deficient (PSEN1/2$^{-/-}$) mouse embryonic fibroblasts (MEFs) (Herreman et al., 2000) were cultured in Dulbecco's modified Eagle's medium/F-12 containing 10% fetal

bovine serum. MEFs were transduced using pMSCV-puro, a replication defective recombinant retroviral expression system (Takara Bio Inc.) harboring cDNA inserts coding for human wild-type (WT) or mutant PSEN1s, carrying either the deletion of exon 9 (Δ9-PSEN1) or the deletion of exons 9 and 10 (Δ9-10-PSEN1). Stable cell lines were selected using 5µg/mL puromycin (Sigma-Aldrich).

Expression and purification of APP-C99-3xFLAG

Substrate purification was performed as previously described (Chávez-Gutiérrez et al., 2008). Purity was assessed by SDS-PAGE followed by Coomassie staining (GelCode reagent, Pierce).

***In Vitro* Activity Assays using Detergent Extracted γ-Secretase Complexes**

In vitro activity assays were performed as previously described (Chávez-Gutiérrez et al., 2008) with minor modifications. Briefly, MEF's microsomal fractions were solubilized in 1% CHAPSO. *In vitro* reactions were carried out in 20 mM Pipes (pH 7.4), 0.15 M NaCl, 0.2 M Sucrose, 1 mM EGTA, 1X EDTA-free complete protease inhibitors (Roche), 2.5% DMSO, 1% phosphatidylcholine and 0.25% CHAPSO. Reactions were incubated for 4 hr at 37°C with 1.75 µM APP-C99-3xFLAG substrate. The γ-secretase inhibitor "Inhibitor X" was purchased from EMD Millipore.

Cell-based assay and Enzyme-Linked ImmunoSorbent Assay

WT and mutant *PSEN1*-rescued MEF cell lines were transduced with the recombinant adenovirus Ad5/CMV-APP bearing human WT-APP695 as previously described (Chávez-Gutiérrez et al., 2008). Medium was refreshed seven hours after transduction and extracellular media were collected 24 hours later. Aβ38, Aβ40 and Aβ42 levels in extracellular media were

quantified on Multi-Spot 96-well plates precoated with anti-Aβ38, -Aβ40 and -Aβ42 using MSD technologies (Haryana, India) as previously described (Szaruga et al., 2015). Aβ43 levels were measured using an Aβ43 ELISA kit (IBL, Männedorf, Switzerland).

RESULTS

Detection and validation of a *PSEN1* exon 9/10 deletion

Apart from a recurrent duplication of the *MAPT* locus and a deletion of the *ABCA7* gene (Le Guennec et al., 2016b), the analysis CNVs by CANOES in the 522 EOAD cases and 584 controls revealed a deletion of exon 9 and 10 of *PSEN1* in patient EXT-313-001. QMPSF experiments confirmed the presence of the genomic deletion (Figure 1A). Additional QMPSF assays were designed to delineate the boundaries of the deletion, using amplicons located in introns 8 and 10 of *PSEN1*. On the basis of these results, PCR amplification and sequencing of the deleted fragment showed that the size of the deletion was 10.1 kb and that the two breakpoints were situated within a 24 bp homologous sequence located in introns 8 and 10, 1 kb distal from exon 9 and 3.4 kb proximal from exon 10, respectively (Figure 1B). *In silico* analysis, using the Repeat Masker program (http://www.repeatmasker.org/), revealed that the rearrangement resulted from a homologous Alu-mediated recombination, the Alu elements spanning the breakpoints deriving from the Alu Y and Alu-Sx subfamily. Skipping of exons 9 and 10 of *PSEN1* is predicted to result in an in-frame deletion, but introduces a S290W missense mutation at the aberrant exon 8-11 junction. RT-PCR experiments on RNA extracted from patient's blood confirmed the expression of the deleted allele (Figure 1C), approximately to the same level as the wild-type allele (Figure 1D). Taken together, we retained the following mutation nomenclature: Chr14(GRCh37):g.73671948_73682054del; NM_000021.3(PSEN1):c.869-1146_1130-1780del; p.Ser290_Arg377delinsTrp;

r.869_1129del, and the following Alu sequence identity: Intron8 g.73671924_g.73671947 Intron10 g.73682031_g.73682054.

Case report

The patient presented with progressive cognitive decline associated with spastic paraparesis from the age of 56 years. **He had no personal medical history. His mother died after a ten-year course of dementia starting from the age of 50 years. No biomaterials were available for the relatives.** Upon examination at age 59, the patient presented spasticity of the lower limbs with decreased motor strength of the left lower limb, pyramidal signs in all four limbs but no upper limb motor deficit. Dystonia as well as extrapyramidal hypertonia of the left hand were noted. Mini Mental State Examination scored 22/30, and he presented severe episodic memory impairment characterized by failure to encode words during the assessment of the free and cued selective reminding test. **Frontal assessment battery revealed executive function disabilities (score was 12/18)** CSF was obtained by lumbar puncture and collected and stored in polypropylene tubes. All three CSF AD biomarkers were consistent with an AD signature: decreased Aβ42 (153 pg/mL, N>700), increased Total-Tau (414 pg/mL, N<350) and Phosphorylated-Tau (64 pg/mL, N<60). Cerebral MRI showed severe atrophy predominantly involving the occipital-parietal bilateral cortex in T1-weighted sequences. A similar volume loss was found in the medial temporal structures**. The cerebral fluorodesoxyglucose positron emission tomography (FDG-PET) revealed a severe hypometabolism affecting the frontal and occipito-parietal bilateral cortex.** No arguments were found for a cerebrovascular disease or cerebral amyloid angiopathy, as only rare unspecific periventricular hyperintensities were present in the FLAIR sequence and T2*-weighted images did not reveal any micro or macro hemorrhage.

Deletion of exons 9-10 drastically impacts the endopeptidase and carboxypeptidase-like activities of PSEN1

To analyze the effect(s) of the deletion of exons 9 and 10 of *PSEN1* (hereafter referred to as Δ9-10 deletion) on γ-secretase activity, Psen1/2$^{-/-}$ MEFs were rescued with human WT or Δ9-10 PSEN1. For comparison purposes, we simultaneously analyzed the well-characterized Δ9 *PSEN1* deletion (Chávez-Gutiérrez et al., 2012) and used the dKO as a negative control.

Apart from PSEN, a mature and active γ-secretase complex is made up of three additional subunits: Nicastrin (NCT), PSEN enhancer 2 (Pen-2) and anterior pharynx 1 (Aph1).

During the assembly and maturation of the γ-secretase complex, PSEN undergoes endoproteolytic cleavage within exon 9, releasing the N- and C-terminal fragments (Lee et al., 1997). As Δ9, the Δ9-10 PSEN1 is not processed and only full-length mutant PSEN1 could be observed on western blot (Figure 2A). The PSEN1-CTF antibody did not stain the Δ9-10 mutant because it targets the PSEN1 loop, encompassing exons 9 and 10. However, the presence of mature Nicastrin (NCT) and Pen-2 at similar levels in the WT and mutant conditions strongly indicates that the mutant Δ9-10 PSEN1 still reconstitutes mature γ-secretase complexes.

To assess the effects of the Δ9-10 deletion, the endopeptidase activity was evaluated in *in vitro* γ-secretase activity assays, using CHAPSO-solubilized membranes prepared from the WT and mutant MEF lines as source of enzyme, and purified APP-C99-3XFlag as substrate. Western blot analysis revealed a strong decrease of AICD-3XFlag staining with both Δ9 and Δ9-10 PSEN1 compared to WT (Figure 2B). These data indicate that both Δ9 and Δ9-10 deletions severely compromise the global endopeptidase protease activity.

With regard to the carboxypeptidase-like γ-secretase function, its efficiency was determined in cell-based experiments by ELISA measurement of secreted Aβ isoforms. Expression of both Δ9 and Δ9-10 PSEN1 resulted in dramatic reductions of Aβ38, Aβ40 and Aβ42 but

increased Aβ43 peptide levels compared to WT (Figure 2C). Remarkably, the exon 9-10 deletion displayed a higher impact on the carboxypeptidase activity than the Δ9 variant, with absence of detectable Aβ38 peptide and stronger reductions in Aβ40 and Aβ42 levels. Mutant Aβ product profiles highlight Aβ43 as the major secreted peptide from the Δ9-10 PSEN1 cell line (Figure 2D). The extreme effect of the Δ9-10 PSEN1 deletion on the carboxypeptidase γ-secretase efficiency is better appreciated while analyzing the Aβ40/Aβ43 ratio, which informs about the efficiency of the 4th catalytic cleavage that converts Aβ43 into Aβ40 (Figure 2E).

DISCUSSION

While searching for copy-number variations using exome sequencing data from patients with EOAD, we identified a novel genomic deletion overlapping exons 9 and 10 of the *PSEN1* gene, resulting from an Alu-mediated recombination. This in-frame deletion led to the production of a **shorter** isoform of PSEN1 lacking exons 9 and 10, which was found to be expressed in patient's blood at a similar level compared to the WT PSEN1. The Δ9-10 PSEN1 variant misses the largest intracellular loop that connects the transmembrane domains VI and VII that contain the catalytic aspartates of the γ-secretase complex, D257 and D384.

The patient carrying the Δ9-10 deletion presented progressive cognitive decline characterized by impaired episodic memory associated with frontal clinical and imaging signs. Evidence of an AD pathophysiological process was provided by all three CSF AD biomarkers. Such situation highlights the importance of exploring AD CSF biomarkers for any patient with a behavioral fronto-temporal dementia according to current criteria (Rascovsky et al., 2011). Cognitive impairment was associated with spastic paraparesis, a common feature observed in patients carrying deletions of the single exon 9 of *PSEN1* and usually associated with cotton-wool plaques at neuropathological examination. The patient had a disease onset at 56 years, while his mother was affected at age 50. In this family, ages

of onset are within the same ranges as the *PSEN1* Δ9 mutation carriers (Karlstrom et al., 2008). Δ9-associated phenotypes are however known to be highly variable (Karlstrom et al., 2008), even between individuals from the same pedigree (Smith et al., 2001).

To assess the consequences of the novel PSEN1 deletion on the function of the γ-secretase complex, we performed *in vitro* cell-free and cell-based γ-secretase activity assays.

Similar to the Δ9 form, the lack of exons 9 and 10 precluded the auto-endoproteolytic cleavage of PSEN1 into NTF and CTF. However, the presence of Pen-2 and mature NCT in both Δ9 and Δ9-10 PSEN1-mutant γ-secretase complexes is a strong indication of complex assembly and maturation.

Subsequent analysis of AICD and Aβ levels revealed that the Δ9-10 PSEN1-mutant strongly impairs the endopeptidase activity and drastically reduces the efficiency of the carboxypeptidase-like cleavages. The effects are indicative of a dysfunction of the γ-secretase complex (Chávez-Gutiérrez et al., 2012). Interestingly, the *PSEN1*- Δ9 and Δ9-10 mutants impact similarly the endopeptidase activity, but differ regarding their effect on carboxypeptidase-like activity.

The Δ9-10 allele induces a prominent shift towards production of the longer Aβ43 peptide as demonstrated by the decreased Aβ40/Aβ43 ratio in cell-based analyses. In fact, Aβ43 is the major peptide secreted from the mutant. Aβ43 has been shown to be potently amyloidogenic and neurotoxic *in vivo* (Saito et al., 2011). Recent data functionally evaluating other extremely inactivating AD-linked *PSEN1* variations show that, as the Δ9-10 mutant, these pathogenic variants elevate Aβ43 secretion compared to the WT allele, supporting the idea that the Aβ43 peptide is a disease-relevant specie, even at low concentrations (Veugelen et al., 2016).

This work further highlights the involvement of deletions hitting the hydrophilic loop of PSEN1, mainly encoded by exons 9 and 10, in EOAD determinism

The pathogenic Δ9 deletion leads to decreased endopeptidase activity, associated with a change of carboxypeptidase-like activity illustrated by an increased Aβ42/Aβ38 ratio (Chávez-Gutiérrez et al., 2012), while the artificial deletion of exon 10 alone affected the carboxypeptidase-like activity of γ-secretase by increasing Aβ42 levels, without impairing the endopeptidase function (Wanngren et al., 2010). Thus, our data suggest a synergistic effect for the Δ9-10 deletion that translates into very low global endopeptidase levels and drastic changes in Aβ profiles. However, our studies cannot exclude that the effects are fully or partially driven by the missense S290W variation at the exon 8-11 junction, as previous work suggested that the effect linked to the deletion of *PSEN1* exon 9 was mostly due to the presence of the missense S290C variation at the aberrant exon8-10 junction (Steiner et al., 1999).

Addressing the mechanistic bases of the differential effects observed for the Δ9, Δ10 and Δ9-10 mutants on γ-secretase function may offer key insights into how the complex protease is regulated. Of note, the recent γ-secretase structure in complex with the inhibitor DAPT (Bai et al., 2015) shows the Tyr288 and the Gly378 at about 6Å from each other; a linker comprised of Ser289 and Trp290 connects these two residues in the Δ9-10 PSEN1 structure (see Figure 2F). Thus, this particular structure puts closely in the space the exons 8 and 11, and may be used to understand the effects of the Δ9-10 mutation on the protease complex.

In conclusion, we describe in an EOAD patient a novel deletion of the *PSEN1* gene encompassing both exons 9 and 10, thus resulting in a complete removal of the largest intracellular hydrophilic loop. The large deletion, encompassing 87 amino acids, does not affect the assembly of a mature protease complex but has an extreme impact on its endopeptidase activity. Interestingly, the mutant carboxypeptidase-like activity is also strongly impaired and the deleterious mutant effect leads to an incomplete digestion of long

Aβ peptides and enhances the production of toxic, aggregation-prone Aβ43. In fact, Aβ43 is the main peptide released from the Δ9-10 PSEN1. These results supports the idea that, as encountered in most EOAD-linked *PSEN1* mutations (Chávez-Gutiérrez et al. 2012), AD-linked *PSEN1* mutations consistently result in impaired carboxypeptidase-like activity and most importantly underlines a potential contribution of Aβ43 to AD pathogenesis.

Genetically, our work (i) further extents the mutation spectrum of EOAD, (ii) demonstrates that exons 9 and 10, that are devoid of pathological missense mutations, are sensitive to deletions, and (iii) underlines the need to independently screen deletions of exons 9 and 10 in familial EOAD cases.

Acknowledgements

This study was funded by grants from the Clinical Research Hospital Program from the French Ministry of Health (GMAJ, PHRC 2008/067), the CNR-MAJ and the JPND PERADES (ANR-13-JPRF-0001-04). Kilan Le Guennec benefited from an EMBO short-term fellowship. This work was also funded by the Stichting Alzheimer Onderzoek (SAO), the Fund for Scientific Research, Flanders, the KU Leuven, a Methusalem grant from the KU Leuven, the Flemish Government and Interuniversity Attraction Poles Program of the Belgian Federal Science Policy Office.

Competing interest

We report no competing interest.

References

Backenroth D, Homsy J, Murillo LR, Glessner J, Lin E, Brueckner M, Lifton R, Goldmuntz E, Chung WK, Shen Y. 2014. CANOES: detecting rare copy number variants from whole exome sequencing data. Nucleic Acids Res 42:e97.

Bai X, Rajendra E, Yang G, Shi Y, Scheres SHW. 2015. Sampling the conformational space of the catalytic subunit of human γ-secretase. eLife 4:.

Chávez-Gutiérrez L, Bammens L, Benilova I, Vandersteen A, Benurwar M, Borgers M, Lismont S, Zhou L, Van Cleynenbreugel S, Esselmann H, Wiltfang J, Serneels L, et al. 2012. The mechanism of γ-Secretase dysfunction in familial Alzheimer disease. EMBO J 31:2261–2274.

Chávez-Gutiérrez L, Tolia A, Maes E, Li T, Wong PC, Strooper B de. 2008. Glu(332) in the Nicastrin ectodomain is essential for gamma-secretase complex maturation but not for its activity. J Biol Chem 283:20096–20105.

Herreman A, Serneels L, Annaert W, Collen D, Schoonjans L, De Strooper B. 2000. Total inactivation of gamma-secretase activity in presenilin-deficient embryonic stem cells. Nat Cell Biol 2:461–462.

Hiltunen M, Helisalmi S, Mannermaa A, Alafuzoff I, Koivisto AM, Lehtovirta M, Pirskanen M, Sulkava R, Verkkoniemi A, Soininen H. 2000. Identification of a novel 4.6-kb genomic deletion in presenilin-1 gene which results in exclusion of exon 9 in a Finnish early onset Alzheimer's disease family: an Alu core sequence-stimulated recombination? Eur J Hum Genet EJHG 8:259–266.

Jurisch-Yaksi N, Sannerud R, Annaert W. 2013. A fast growing spectrum of biological functions of γ-secretase in development and disease. Biochim Biophys Acta 1828:2815–2827.

Karlstrom H, Brooks WS, Kwok JBJ, Broe GA, Kril JJ, McCann H, Halliday GM, Schofield PR. 2008. Variable phenotype of Alzheimer's disease with spastic paraparesis. J Neurochem 104:573–583.

Le Guennec K, Nicolas G, Quenez O, Charbonnier C, Wallon D, Bellenguez C, Grenier-Boley B, Rousseau S, Richard A-C, Rovelet-Lecrux A, Bacq D, Garnier J-G, et al. 2016a. ABCA7 rare variants and Alzheimer disease risk. Neurology 86:2134–2137.

Le Guennec K, Quenez O, Nicolas G, Wallon D, Rousseau S, Richard A-C, Alexander J, Paschou P, Charbonnier C, Bellenguez C, Grenier-Boley B, Lechner D, et al. 2016b. 17q21.31 duplication causes prominent tau-related dementia with increased MAPT expression. Mol Psychiatry.

Lee MK, Borchelt DR, Kim G, Thinakaran G, Slunt HH, Ratovitski T, Martin LJ, Kittur A, Gandy S, Levey AI, Jenkins N, Copeland N, et al. 1997. Hyperaccumulation of FAD-linked presenilin 1 variants in vivo. Nat Med 3:756–760.

McKhann GM, Knopman DS, Chertkow H, Hyman BT, Jack CR, Kawas CH, Klunk WE, Koroshetz WJ, Manly JJ, Mayeux R, Mohs RC, Morris JC, et al. 2011. The diagnosis of dementia due to Alzheimer's disease: recommendations from the National Institute on Aging-Alzheimer's Association workgroups on diagnostic guidelines for Alzheimer's disease. Alzheimers Dement J Alzheimers Assoc 7:263–269.

Nicolas G, Charbonnier C, Wallon D, Quenez O, Bellenguez C, Grenier-Boley B, Rousseau S, Richard A-C, Rovelet-Lecrux A, Le Guennec K, Bacq D, Garnier J-G, et al. 2016a. SORL1 rare variants: a major risk factor for familial early-onset Alzheimer's disease. Mol Psychiatry 21:831–836.

Nicolas G, Wallon D, Charbonnier C, Quenez O, Rousseau S, Richard A-C, Rovelet-Lecrux A, Coutant S, Le Guennec K, Bacq D, Garnier J-G, Olaso R, et al. 2016b. Screening of dementia genes by whole-exome sequencing in early-onset Alzheimer disease: input and lessons. Eur J Hum Genet EJHG 24:710–716.

Perez-Tur J, Froelich S, Prihar G, Crook R, Baker M, Duff K, Wragg M, Busfield F, Lendon C, Clark RF. 1995. A mutation in Alzheimer's disease destroying a splice acceptor site in the presenilin-1 gene. Neuroreport 7:297–301.

Prihar G, Verkkoniem A, Perez-Tur J, Crook R, Lincoln S, Houlden H, Somer M, Paetau A, Kalimo H, Grover A, Myllykangas L, Hutton M, et al. 1999. Alzheimer disease PS-1 exon 9 deletion defined. Nat Med 5:1090.

Rascovsky K, Hodges JR, Knopman D, Mendez MF, Kramer JH, Neuhaus J, Swieten JC van, Seelaar H, Dopper EGP, Onyike CU, Hillis AE, Josephs KA, et al. 2011. Sensitivity of revised diagnostic criteria for the behavioural variant of frontotemporal dementia. Brain J Neurol 134:2456–2477.

Rovelet-Lecrux A, Charbonnier C, Wallon D, Nicolas G, Seaman MNJ, Pottier C, Breusegem SY, Mathur PP, Jenardhanan P, Le Guennec K, Mukadam AS, Quenez O, et al. 2015. De novo deleterious genetic variations target a biological network centered on Aβ peptide in early-onset Alzheimer disease. Mol Psychiatry 20:1046–1056.

Rovelet-Lecrux A, Hannequin D, Raux G, Le Meur N, Laquerrière A, Vital A, Dumanchin C, Feuillette S, Brice A, Vercelletto M, Dubas F, Frebourg T, et al. 2006. APP locus duplication causes autosomal dominant early-onset Alzheimer disease with cerebral amyloid angiopathy. Nat Genet 38:24–26.

Saito T, Suemoto T, Brouwers N, Sleegers K, Funamoto S, Mihira N, Matsuba Y, Yamada K, Nilsson P, Takano J, Nishimura M, Iwata N, et al. 2011. Potent amyloidogenicity and pathogenicity of Aβ43. Nat Neurosci 14:1023–1032.

Sato S, Kamino K, Miki T, Doi A, Ii K, St George-Hyslop PH, Ogihara T, Sakaki Y. 1998. Splicing mutation of presenilin-1 gene for early-onset familial Alzheimer's disease. Hum Mutat Suppl 1:S91-94.

Smith MJ, Kwok JB, McLean CA, Kril JJ, Broe GA, Nicholson GA, Cappai R, Hallupp M, Cotton RG, Masters CL, Schofield PR, Brooks WS. 2001. Variable phenotype of Alzheimer's disease with spastic paraparesis. Ann Neurol 49:125–129.

Steiner H, Romig H, Grim MG, Philipp U, Pesold B, Citron M, Baumeister R, Haass C. 1999. The biological and pathological function of the presenilin-1 Deltaexon 9 mutation is independent of its defect to undergo proteolytic processing. J Biol Chem 274:7615–7618.

Szaruga M, Veugelen S, Benurwar M, Lismont S, Sepulveda-Falla D, Lleo A, Ryan NS, Lashley T, Fox NC, Murayama S, Gijsen H, De Strooper B, et al. 2015. Qualitative changes in human γ-secretase underlie familial Alzheimer's disease. J Exp Med 212:2003–2013.

Takami M, Nagashima Y, Sano Y, Ishihara S, Morishima-Kawashima M, Funamoto S, Ihara Y. 2009. gamma-Secretase: successive tripeptide and tetrapeptide release from the transmembrane domain of beta-carboxyl terminal fragment. J Neurosci Off J Soc Neurosci 29:13042–13052.

Veugelen S, Saito T, Saido TC, Chávez-Gutiérrez L, De Strooper B. 2016. Familial Alzheimer's Disease Mutations in Presenilin Generate Amyloidogenic Aβ Peptide Seeds. Neuron 90:410–416.

Wanngren J, Frånberg J, Svensson AI, Laudon H, Olsson F, Winblad B, Liu F, Näslund J, Lundkvist J, Karlström H. 2010. The large hydrophilic loop of presenilin 1 is important for regulating gamma-secretase complex assembly and dictating the amyloid beta peptide (Abeta) Profile without affecting Notch processing. J Biol Chem 285:8527–8536.

Figure legends

Figure 1. Validation of the *PSEN1* genomic deletion overlapping exon 9 and 10.

A. Quantitative Multiplex PCR of Short Fluorescent fragments (QMPSF). The electropherogram of the patient (red) was superposed to a control subject (blue) by adjusting peak height to the control amplicon *PCBD2*. The vertical axis shows fluorescence in arbitrary units and the horizontal axis represents the size of the different amplicons in base pairs. Arrows indicate the heterozygous deletion detected by a 50% decrease of the corresponding peaks. B. Sanger sequencing of the genomic deleted allele. The breakpoints are located into intron 8 and 10. Double red arrow indicates the 24 base pairs homologous sequence mediating the Alu recombination. C. Sanger sequencing of the cDNA from the deleted allele. D. Amplification of WT and Δ9-10 alleles of PSEN1 by RT-PCR in control individual and patient EXT-313-001. Reverse transcriptions without RNA (-RNA) or polymerase (-enzyme) were used as controls. Arrows indicate the WT and Δ9-10 cDNAs.

Figure 2. Functional analysis of the endopeptidase and carboxypeptidase activities of γ-secretase.

A. Western Blot of γ-secretase components. Nicastrin, PSEN1-NTF, PSEN1-CTF and Pen-2 protein levels in *PSEN1/2*$^{-/-}$ MEFs transduced to express human WT, Δ9 and Δ9-10 PSEN1. Arrowheads indicate full-length forms of Δ9 and Δ9-10 PSEN1. B. Analysis of endopeptidase cleavage. Measurements of AICD level for WT, Δ9 and Δ9-10 PSEN1 γ-secretase complex after *in vitro* activity assay in presence or absence of an active site γ-secretase Inhibitor (InhX). C. Analysis of secreted Aβ38, Aβ40, Aβ42 and Aβ43 in extracellular media by ELISA. D. The corresponding Aβx/total Aβ ratio and E. the corresponding Aβ40/Aβ43 ratio, as an indication of γ-secretase processivity. All experiments were repeated three to eight times. Graphs show mean ± SD and statistical significance was tested with one way ANOVA

and Dunnett's post-test ****, P<0.0001, *** P<0.001). F. Presenilin 3D structure in complex with the inhibitor DAPT (blue) (PDB code: 5FN2). Side chains of active site Asp257 and Asp385 are shown and transmembrane (TM) helices are indicated. Tyr 288 (Y288) and Gly378 (G378) are connected by Ser289 and Trp290 (S289-W290) in the mutant Δ9-10 PSEN1 (indicated by red arrow).

Figure 1

A

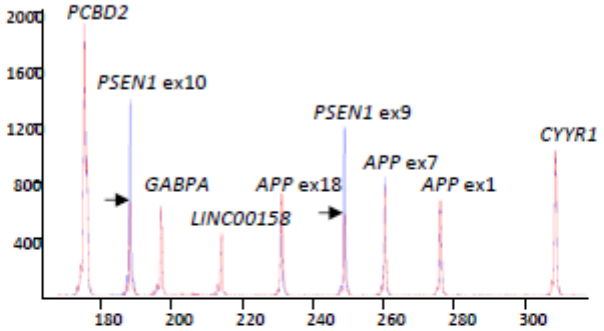

B

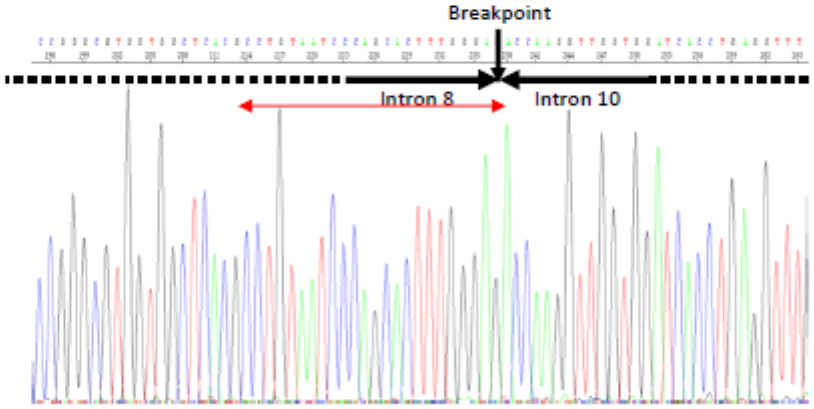

C

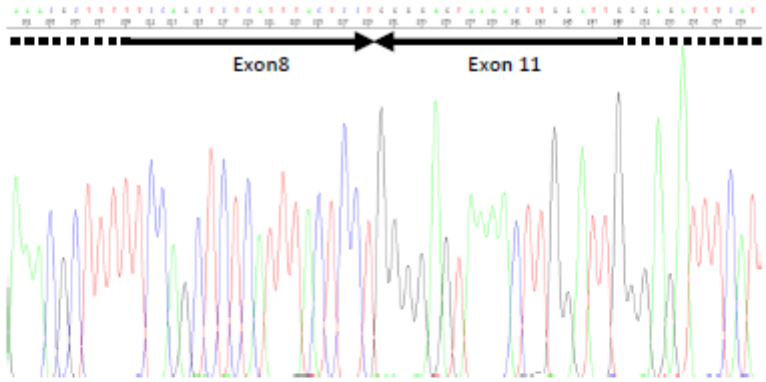

D

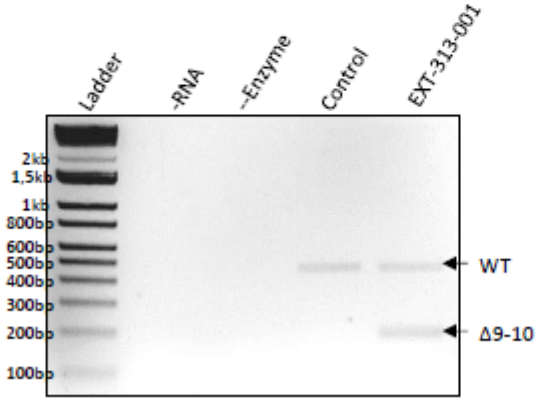

Figure 2

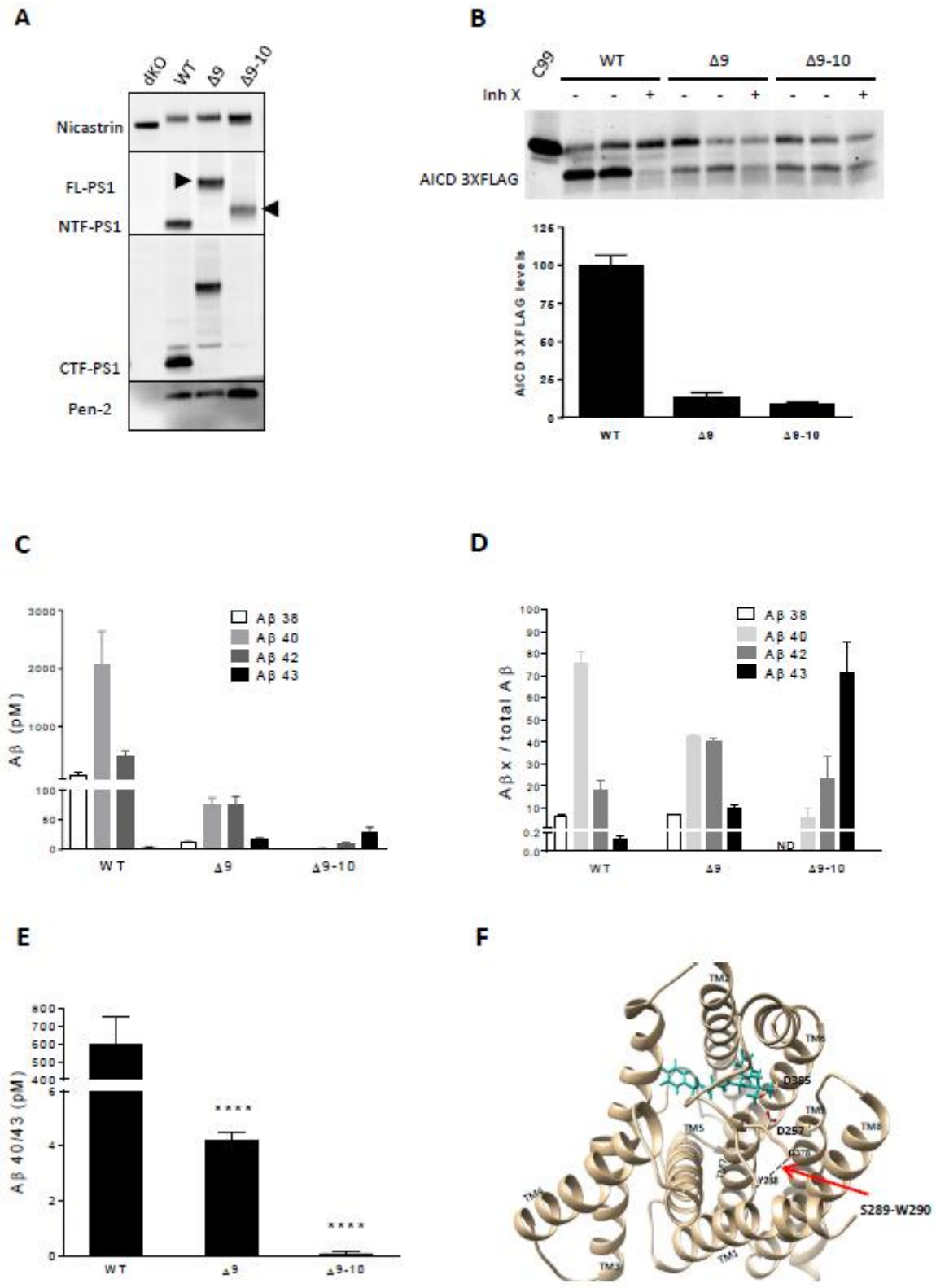

Highlights

- Copy-number variation analysis from exome data in EOAD patients.
- Identification of a genomic deletion of exons 9 and 10 of *PSEN1*.
- This in-frame deletion results in an increased secretion of Aβ43.
- These data support the pathogenic role of Aβ43 EOAD pathophysiology.